DALTON
FULL PAPER

Synthesis and characterisation of two new catechol-based iron(III) ion-sequestering agents

Carla Bazzicalupi,[a] Andrea Bencini,[a] Antonio Bianchi,[a] Vieri Fusi,[b] Claudia Giorgi,[a] Luigi Messori,[a] Marzia Migliorini,[a] Piero Paoletti[a] and Barbara Valtancoli[a]

[a] *Department of Chemistry, University of Florence, via Maragliano 75/77, 50144 Florence, Italy*
[b] *Institute of Chemical Sciences, University of Urbino, Piazza Rinascimento 6, 61026 Urbino, Italy*

The new compounds 1,4,10,13-tetrakis(2,3-dihydroxybenzoyl)-7,16-dimethyl-1,4,7,10,13,16-hexaazacyclooctadecane (H_8L^1) and 1,4,7,10,13,16-hexakis(2,3-dihydroxybenzoyl)-1,4,7,10,13,16-hexaazacyclooctadecane ($H_{12}L^2$), having macrocyclic skeletons bearing four and six catechol hanging groups, respectively, have been synthesized and characterised. The crystal structure of $H_8L^1 \cdot 2dmso \cdot 2H_2O$ (dmso = dimethyl sulfoxide), has been solved by single-crystal X-ray analysis. The equilibrium constants for protonation of the macrocycles and complexation of Fe^{3+} have been studied by potentiometric procedures in water–dmso (50 : 50 v/v), 0.1 mol dm^{-3} NMe_4Cl, at 298.1 ± 0.1 K. Both compounds are able to form mono- and di-nuclear iron(III) complexes of very high stability. These results indicate that the two compounds are thermodynamically able to scavenge Fe^{3+} from iron(III) transferrin. Their effectiveness as scavengers has been demonstrated by spectrophotometric measurements on the transmetallation reactions occurring in the presence of diiron(III) transferrin in aqueous solution. For comparison, the drug desferrioxamine B (DFB) has been also considered under the same experimental conditions. In 0.1 mol dm^{-3} phosphate buffer, at pH 7.4, both H_8L^1 and $H_{12}L^2$ remove iron from diiron(III) transferrin, the transmetallation reactions being much faster for $H_{12}L^2$ than for DFB which is slightly more effective than H_8L^1.

Siderophores are low-molecular mass compounds secreted by micro-organisms for absorbing iron from the environment.[1] Their biosynthesis is promoted by low iron levels and their function is to supply iron to the cells. These naturally occurring ligands, having very high affinity for iron, contain as principal chelating functionalities hydroxamate units (as in ferrichromes and ferrioxamines) or catechol groups (as in enterobactin).[1–4]

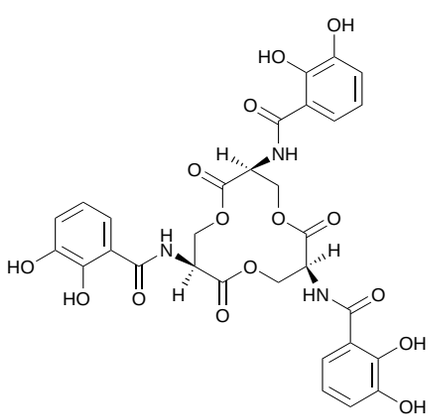

Enterobactin

Enterobactin can be considered the prototype of catechol siderophores. It presents the highest formation constant (log $K = 52$)[5] ever observed for complexes of Fe^{3+} with natural ligands. Its efficiency as iron(III) ion scavenger and carrier has stimulated the synthesis of many analogues containing three catechol units in tripodal or cage-like structures characterised by the same three-fold symmetry.[6–8]

Iron is an essential element for most living organisms,[1,9,10] although it is also very toxic when present in excess. The most common sources of acute human iron poisoning are repeated blood transfusions, as in the treatment of patients affected by Cooley's anaemia (about 3 million world-wide), and misapplications of iron-rich vitamins. Human iron overloads can be reduced by administration of iron sequestering agents which are able to scavenge the metal from the natural stores, such as transferrin and ferritin, converting it into a form that the body can excrete.[3] This is currently achieved by means of the drug desferrioxamine B (Desferal, Ciba). This drug, however, has the drawback of no oral activity and of short body retention time coupled with slowness in iron removal; therefore, daily, or almost daily, disagreeable subcutaneous or intravenous slow perfusions are necessary.

Recent studies demonstrated that iron removal from transferrin,[11] or from the similar protein lactoferrin,[12] is accelerated by mediator anions which modify the protein structure rendering the metal centre more accessible to sequestering agents. In this sense there is evidence that catechol groups behave as mediator anions so that catechol-containing ligands are favoured, from a kinetic point of view, in removing iron bound to these proteins.

In this light, we have synthesized the new compounds H_8L^1 and $H_{12}L^2$, containing large numbers of catechol units (four and six, respectively), and studied their binding properties towards Fe^{3+} as well as their effectiveness in scavenging Fe^{3+} from diiron(III) transferrin. Owing to the insufficient water solubility of these ligands, water–dimethyl sulfoxide (dmso) (50 : 50 v/v, 80 : 20 mol/mol) was employed as a solvent in the potentiometric study involving ligand deprotonation/protonation and Fe^{3+} complexation equilibria. Dimethyl sulfoxide and its mixtures with water are very useful as pure water substitutes for this kind of study.[13] In particular, equilibrium data obtained in water–dmso mixtures with a modest dmso content, like that employed in the present work, are closely comparable with the analogous data determined in pure water. On the other hand the direct competition between the new catechol-based ligands (H_8L^1 and $H_{12}L^2$) and diiron(III) transferrin was performed in water.

Experimental

Synthesis of the ligands

The syntheses of the macrocycles H_8L^1 and $H_{12}L^2$ are outlined in Scheme 1. The macrocycle 1,4,7,10,13,16-hexaazacyclo-

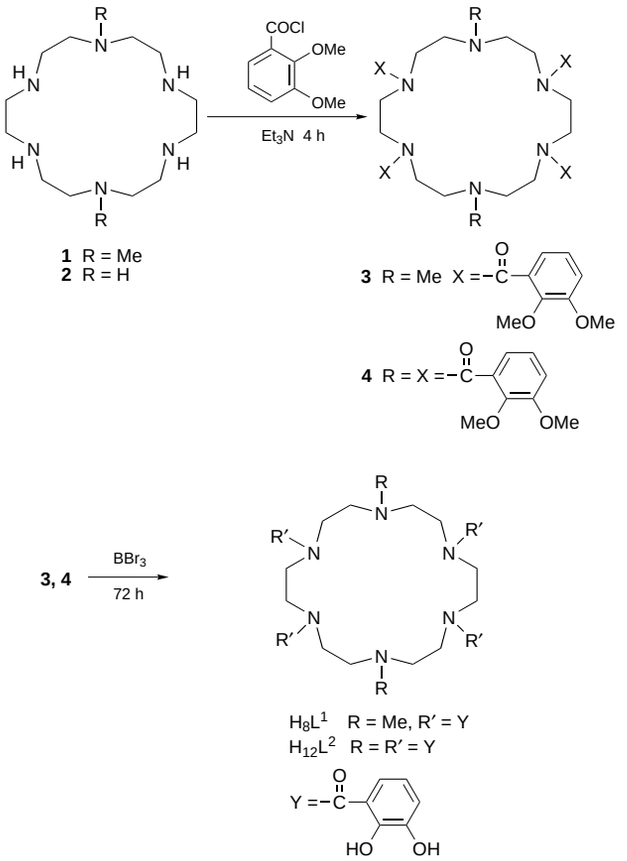

Scheme 1

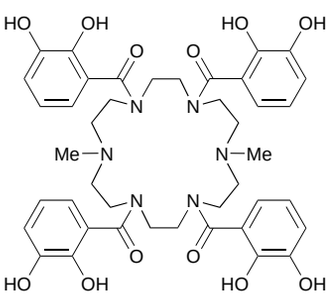

H_8L^1

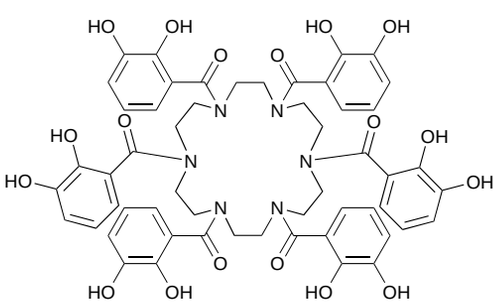

$H_{12}L^2$

octadecane **2** was purchased from Fluka, while 1,10-dimethyl-1,4,7,10,13,16-hexaazacyclooctadecane **1** was synthesized as previously described.[14] All other chemicals (reagent grade) were obtained from different commercial sources and used as delivered.

1,4,10,13-Tetrakis(2,3-dimethoxybenzoyl)-7,16-dimethyl-1,4,7,10,13,16-hexaazacyclooctadecane 3. A mixture of 2,3-dimethoxybenzoic acid (3.57 g, 0.0196 mol) and thionyl chloride (40 g, 0.34 mol) was allowed to react overnight under an inert atmosphere at 35 °C. The excess of thionyl chloride was removed by distillation *in vacuo* at room temperature; the residue was dissolved in dry benzene and the solvent evaporated as before. The last operation was repeated twice,. The product was then dissolved in the minimum volume of dry benzene, under an inert atmosphere, and 1,10-dimethyl-1,4,7,10,13,16-hexaazacyclooctadecane **1** (1.0 g, 0.0035 mol) in dry benzene (40 cm^3) was added dropwise at room temperature over a period of 4 h with stirring. Stirring was maintained for 30 min, the resulting suspension was filtered and the solid residue treated with hot benzene. The suspended solid was filtered off and the hot solution evaporated to dryness. The white residue was dried *in vacuo* at 50 °C; yield 75% (Found: C, 63.5; H, 7.0; N, 8.8. Calc. for $C_{50}H_{66}N_6O_{12}$: C, 63.6; H, 7.05; N, 8.9%).

1,4,10,13-Tetrakis(2,3-dihydroxybenzoyl)-7,16-dimethyl-1,4,7,10,13,16-hexaazacyclooctadecane dihydrobromide (H_8L^1·2HBr). A mixture of compound **3** (1 g, 1.06 mmol), and BBr_3 (25 g, 0.1 mol) in dry chloroform (150 cm^3) was maintained under an inert atmosphere with stirring for 3 d. The resulting yellowish suspension was chilled in a water–ice bath and methanol (300 cm^3) was added dropwise, with great caution, with stirring. The refrigerating bath was then removed and after 30 min the resulting solution was evaporated to dryness *in vacuo*. Several times the brown residue was dissolved in methanol and the solvent evaporated. The product was further purified by crystallisation from ethanol–diethyl ether; yield 20% (Found: C, 50.7; H, 5.3; N, 8.4. Calc. for $C_{42}H_{52}Br_2N_6O_{12}$: C, 50.81; H, 5.28; N, 8.46%).

1,4,7,10,13,16-Hexakis(2,3-dimethoxybenzoyl)-1,4,7,10,13,16-hexaazacyclooctadecane 4. This compound was obtained by adopting a similar procedure to that for **3**; yield 75% (Found: C, 63.7; H, 6.4; N, 6.7. Calc. for $C_{66}H_{78}N_6O_{18}$: C, 63.76; H, 6.32; N, 6.76%).

1,4,7,10,13,16-Hexakis(2,3-dihydroxybenzoyl)-1,4,7,10,13,16-hexaazacyclooctadecane ($H_{12}L^2$). This compound was obtained by adopting a similar procedure to that for H_8L^1·2HBr; yield 43% (Found: C, 60.2; H, 5.1; N, 7.8. Calc. for $C_{54}H_{54}N_6O_{18}$: C, 60.33; H, 5.06; N, 7.82%).

H_8L^1·2dmso·2H_2O. Pale yellow prismatic crystals of this compound suitable for X-ray analysis were obtained by slow diffusion of water into a solution containing H_8L^1·2HBr in dmso.

Crystallography

Crystal data and data collection parameters for H_8L^1·2dmso·2H_2O. $C_{46}H_{66}N_6O_{16}S_2$, $M = 1023.17$, $a = 9.991(4)$, $b = 14.700(10)$, $c = 16.990(10)$ Å, $\beta = 99.07(4)°$, $U = 2464(2)$ Å^3 (by least-squares refinement on diffractometer angles from 25 centred reflections, $16 < 2\theta < 25°$), $T = 298$ K, space group $P2_1/c$, graphite-monochromated Cu-Kα radiation, $\lambda = 1.5418$ Å, $Z = 2$, $D_c = 1.379$ Mg m^{-3}, $F(000) = 1088$, pale yellow prism with approximate dimensions $0.04 \times 0.065 \times 0.10$ mm, $\mu = 1.625$ mm^{-1}, Enraf-Nonius CAD4 diffractometer, θ–2θ scans, data collection range $8 < 2\theta < 130°$, $\pm h, k, l$, two standard reflections showed no loss of intensity; 2740 reflections collected, 1993 unique observed reflections with $I > 2\sigma(I)$. Absorption correction performed by means of the DIFABS[15] program once the structure had been solved.

Structure solution and refinement. The structure was solved by means of direct methods of the SIR 92 program.[16] A disordered molecule of dmso is present in the asymmetric unit (population parameters 0.65 and 0.35 for the S the S′ atom, respectively). Anisotropic displacement parameters were used for all the non-hydrogen atoms. Hydrogen atoms bound to the carbon atoms of the ligand and of the solvent dmso molecule were included in calculated positions and isotropically refined

with an overall thermal parameter. The ΔF map in the last refinement step did not allow us to localise the hydrogen atoms of the catechol OH groups.

At the end of the refinement the final agreement factors for 327 refined parameters were $R = 0.0712$ [$I > 2\sigma(I)$] and $wR2 = 0.2267$ (all data). Refinements were performed by means of the full-matrix least-squares method. The function minimised was $\Sigma w(F_o^2 - F_c^2)^2$ with $w = 1/[\sigma^2(F_o^2) + (0.1238P)^2 + 6.29P]$ and $P = (F_o^2 + 2\ F_c^2)/3$. Refinement calculations, carried out on a DEX 486-DX computer, were performed with the SHELXL 93[17] program, which uses the analytical approximation for the atomic scattering factors and anomalous dispersion corrections for all the atoms from ref. 18.

CCDC reference number 186/811.

See http://www.rsc.org/suppdata/dt/1998/359/ for crystallographic files in .cif format.

Potentiometric measurements

All the pH-metric measurements (pH = $-\log[H^+]$) were carried out in degassed water–dmso (50:50 v/v), 0.1 mol dm^{-3} NMe_4Cl, at 298.1 ± 0.1 K, by using equipment and the methodology described for aqueous solutions.[19] The combined Ingold 405 S7/120 electrode was calibrated as a hydrogen-ion concentration probe by titrating known amounts of HCl with CO_2-free NMe_4OH solutions and determining the equivalence point by Gran's method[20] which allows the determination of the standard potential E° and the ionic product of water [(pK_w = 15.59(1) at 298.1 K in 0.1 mol dm^{-3} NMe_4Cl]. An empirical correction was applied for the liquid-junction potential in very acidic solutions. At least three measurements (about 100 data points each) were performed for each system in the range pH 2.5–13 for the determination of the protonation constants and in the ranges 2.5–5.7 and 2.5–9 for complexation of Fe^{3+} in the presence of H_8L^1 and $H_{12}L^2$, respectively. At higher pH values the complexation reactions were not amenable to analysis due to precipitation [probably of uncharged $Fe(H_5L^1)$ and $Fe_2(H_2L^1)$], in the case of Fe^{3+}–H_8L^1, and to extreme slowness in the attainment of equilibrium conditions in the case of Fe^{3+}–$H_{12}L^2$. Similar inconveniences were also found in water–dmso mixtures with higher percentages of the organic solvent. In all experiments the macrocycle concentration [L] (L = H_8L^1 or $H_{12}L^2$) was about 1×10^{-3} mol dm^{-3}, while in the complexation measurements the metal-ion concentration [M] was varied in the range [L] ≤ [M] ≤ 3[L]. Hydrolysis of Fe^{3+} was investigated potentiometrically in the present medium, in this work, leading to the equilibrium constants (included in complexation constant calculations): log $K = -2.81(1)$ for $Fe^{3+} + H_2O \rightleftharpoons [Fe(OH)]^{2+} + H^+$ and $-5.59(1)$ for $Fe^{3+} + 2H_2O \rightleftharpoons [Fe(OH)_2]^+ + 2H^+$.

The computer program HYPERQUAD[21] was used to calculate both protonation and complex-formation constants from electromotive force data. Owing to the great number of species formed at equilibrium, great care was taken in the selection of the equilibrium models according to the procedure reported in footnote 18 of ref. 19(*b*).

Electronic spectra

Electronic spectra in the UV/VIS region were recorded on a Cary 3 Varian instrument operating at room temperature. Samples were *ca.* 1×10^{-4} mol dm^{-3} in the iron complex. For comparison purposes the spectrum of the tris(catecholato)-iron(III) complex was also recorded.

Iron-scavenging studies

Diiron(III) transferrin was prepared by saturation of apotransferrin with iron(III) chloride; apotransferrin solutions 1×10^{-4} mol dm^{-3} in protein, pH 7.4, were treated with 2 equivalents of iron(III) chloride in the presence of a four-fold excess of sodium hydrogencarbonate. Formation of diiron(III) transferrin is accompanied by its characteristic red-orange colour. Complex formation was then confirmed by spectrophotometric analysis by measuring the absorbance ratio at 465 and 280 nm. Iron-removal studies were performed by treating the diiron(III) transferrin samples with an excess of H_8L^1 and $H_{12}L^2$, either in 0.1 mol dm^{-3} Na_2SO_4 or in 0.1 mol dm^{-3} phosphate buffer, and by monitoring the time dependence of the reaction at 293 K using a J500C JASCO dichrograph over several hours. The decrease in molar ellipticity at 450 nm corresponds to the extraction of iron from the specific protein binding sites. For comparison parallel experiments with desferrioxamine B as iron chelator were carried out.

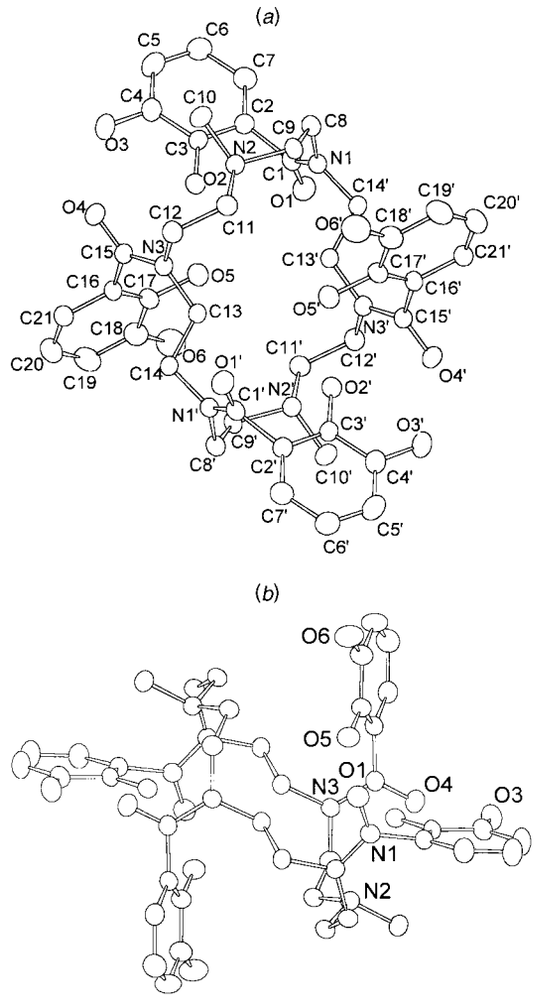

Fig. 1 Molecular structure of H_8L^1 in $H_8L^1 \cdot 2dmso \cdot 2H_2O$. (*a*) Top view, (*b*) lateral view. Symmetry transformation: $2 - x, -y, -z$

Results and Discussion

Synthesis

The synthetic procedure to obtain $H_8L^1 \cdot 2HBr$ and $H_{12}L^2$ is sketched in Scheme 1. Reaction of the macrocycle **1**[13] and 2,3-dimethoxybenzoyl chloride was carried out in benzene at room temperature and affords product **3** in rather good yield. Deprotection of the methylated catechol groups was carried out by using a large excess of BBr_3. The unreacted BBr_3 was treated with methanol. The methyl borate ester formed was removed by vacuum evaporation to leave $H_8L^1 \cdot 2HBr$. The $H_{12}L^2$ macrocycle was obtained by using a similar procedure. Treatment of **2** with 2,3-dimethoxybenzoyl chloride yields **4**, which was subsequently demethylated by using BBr_3.

Crystal structure

The crystal structure of $H_8L^1 \cdot 2dmso \cdot 2H_2O$ consists of H_8L^1

Table 1 Selected bond lengths (Å) and angles (°) for $H_8L^1 \cdot 2dmso \cdot 2H_2O$

N1–C1	1.356(8)	N2–C11	1.508(8)
N1–C14′	1.468(8)	C11–C12	1.520(9)
N1–C8	1.464(8)	C12–N3	1.464(8)
C1–O1	1.232(8)	N3–C15	1.367(8)
C1–C2	1.502(9)	N3–C13	1.475(8)
C2–C7	1.396(10)	C13–C14	1.525(9)
C2–C3	1.385(9)	C15–O4	1.234(8)
C3–O2	1.337(7)	C15–C16	1.497(9)
C3–C4	1.409(10)	C16–C17	1.376(9)
C4–O3	1.368(9)	C16–C21	1.390(9)
C4–C5	1.376(10)	C17–O5	1.373(8)
C5–C6	1.366(12)	C17–C18	1.419(10)
C6–C7	1.375(11)	C18–O6	1.361(10)
C8–C9	1.503(9)	C18–C19	1.378(11)
C9–N2	1.521(8)	C19–C20	1.371(12)
N2–C10	1.490(8)	C20–C21	1.380(11)
C1–N1–C14′	118.5(5)	N2–C11–C12	113.9(5)
C1–N1–C8	123.9(6)	N3–C12–C11	113.7(5)
C14′–N1–C8	117.5(5)	C15–N3–C12	119.7(6)
O1–C1–N1	121.0(6)	C15–N3–C13	123.1(5)
O1–C1–C2	120.1(6)	C12–N3–C13	117.1(5)
N1–C1–C2	118.8(6)	N3–C13–C14	115.2(5)
C7–C2–C3	121.2(7)	N1′–C14–C13	108.5(5)
C7–C2–C1	122.7(7)	O4–C15–N3	121.1(6)
C3–C2–C1	116.0(6)	O4–C15–C16	119.9(6)
O2–C3–C4	118.3(6)	N3–C15–C16	118.8(6)
O2–C3–C2	123.1(6)	C17–C16–C21	120.4(7)
C4–C3–C2	118.5(6)	C17–C16–C15	122.8(6)
O3–C4–C5	122.2(7)	C21–C16–C15	116.8(7)
O3–C4–C3	118.4(7)	O5–C17–C16	125.0(6)
C5–C4–C3	119.3(7)	O5–C17–C18	115.2(7)
C4–C5–C6	121.4(8)	C16–C17–C18	119.8(7)
C7–C6–C5	120.5(8)	O6–C18–C19	120.8(8)
C6–C7–C2	119.0(8)	O6–C18–C17	120.6(7)
N1–C8–C9	115.9(6)	C19–C18–C17	118.6(8)
C8–C9–N2	113.9(5)	C20–C19–C18	121.2(8)
C10–N2–C11	111.8(5)	C19–C20–C21	120.5(8)
C10–N2–C9	110.7(5)	C20–C21–C16	119.6(8)
C11–N2–C9	109.1(5)		

Symmetry transformations used to generate equivalent atoms: $2 - x, -y, -z$.

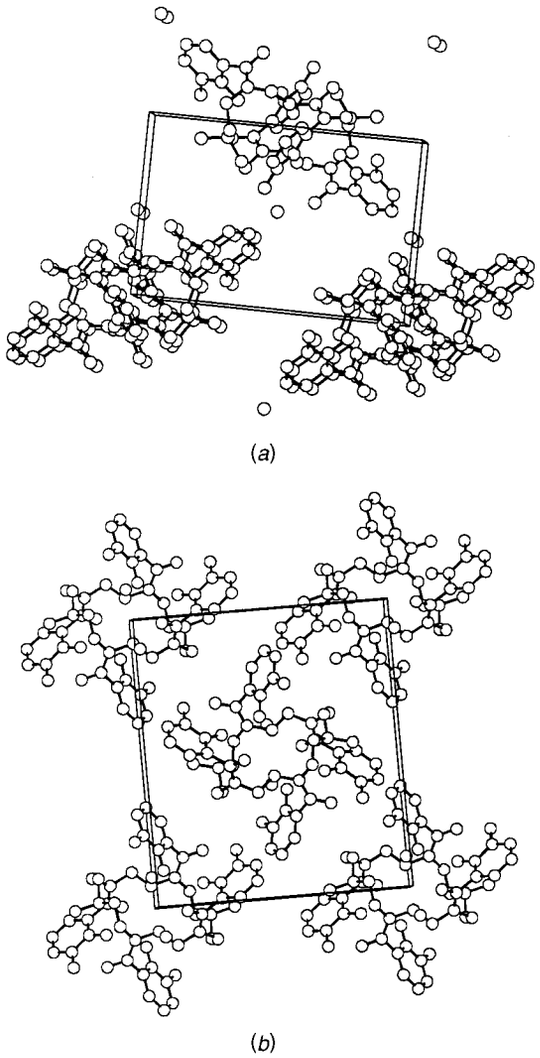

Fig. 2 Crystal packing of $H_8L^1 \cdot 2dmso \cdot 2H_2O$ without the disordered dmso molecules. (*a*) Down the *c* axis, (*b*) down *a*

discrete molecules, dmso and water solvent molecules. Fig. 1 shows an ORTEP[22] drawing of the molecule with atom labelling and bond lengths and angles are reported in Table 1. The molecule is disposed around a crystallographic inversion centre.

The macrocyclic framework assumes a chair conformation defining an internal surface of approximate dimensions 5 × 7 Å. The values of the bond angles reveal the presence of conformational stress due to the four side-groups. In particular, the carbon atoms bound to the N1 and N3 amidic nitrogen atoms present the most remarkable shifts from the theoretical sp^3 hybridisation [N1–C8–C9 115.9(6), C11–C12–N3 113.7(5) and N3–C13–C14 115.2(5)°]. On the other hand, the C14 carbon atom, also bound to N1, shows an angular value of 108.5(5)°, equal within the standard deviation to that required for the sp^3 hybridisation. The lower degree of strain shown by this carbon atom is probably explained by the torsional angular values C8–N1–C1–O1 [−168.5(6)] and C14–N1′-C1′-O1′ [−6.9(9)°] which deviate significantly from the theoretical ones for amidic nitrogens (0, 180°) compared with C12–N3–C15–O4 [−0.7(9)] and C13–N3–C15–O4 [−176.6(6)°]. The lower strain is connected to a loss of conjugation ability.

The carbonylic groups are not coplanar with the aromatic rings [O1–C1–C2–C7 69.9(9) and O4–C15–C16–C21 61.0(9)°], and the two aromatic rings in the asymmetric unit are almost normal to each other, their dihedral angle being 85.3(7)°. This disposition brings the oxygens and the methylated nitrogen N2 so close to each other that the presence of a strong hydrogen-bond interaction seems likely [O1 · · · O5 3.662(7), O2 · · · N2 2.586(6), O2 · · · O4 3.035(7), O2 · · · O5 2.455(6), O3 · · · O4 2.878(7) Å]. Unfortunately, the diffraction data are not good enough to allow the determination of the positions of the four hydrogen atoms involved in these interactions. Since the localisation of such protons is doubtful, due to the possibility of zwitterionic structures, protons were not introduced in calculated positions.

Some other significant hydrogen-bond contacts are formed by the O7 oxygen belonging to the water molecule, which actually bridges two symmetry-related H_8L^1 molecules [O7 · · · O1′ 2.776(9), O7 · · · O1″ 2.865(8), O7 · · · O5″ 2.980(8), O7 · · · O6″ 2.74(1) Å]. Fig 2(*a*) shows a view of the crystal packing (without the disordered dmso molecules) along the lattice direction *c* where the water molecules, lying in free channels between the ligand molecules, are clearly recognisable. In Fig. 2(*b*) a different view, along direction *a*, shows the superimposed ligand molecules giving rise to channels which develop along this crystallographic axis.

Ligand protonation equilibria

The logarithms of the protonation constants of $(L^1)^{8-}$ and $(L^2)^{12-}$ determined by potentiometric titration in 0.1 mol dm^{-3} NMe_4Cl in water–dmso (50 : 50 v/v) solution at 298.1 ± 0.1 K, in the range pH 2.5–13.5, are listed in Table 2.

The principal characteristics of these compounds is their very high basicity, due to the presence of a large number of catechol groups. Actually, the protonation constants of the

Table 2 Logarithms of the protonation constants of $(L^1)^{8-}$ and $(L^2)^{12-}$ determined in water–dmso (50 : 50 v/v), 0.1 mol dm^{-3} NMe_4Cl, at 298.1 ± 0.1 K

Reaction	log *K*	Reaction	log *K*
$(H_2L^1)^{6-} + 2H^+ \rightleftharpoons (H_4L^1)^{4-}$	26.35(3)*	$(H_3L^2)^{9-} + 3H^+ \rightleftharpoons (H_6L^2)^{6-}$	39.78(3)
$(H_2L^1)^{6-} + 3H^+ \rightleftharpoons (H_5L^1)^{3-}$	37.24(6)	$(H_3L^2)^{9-} + 4H^+ \rightleftharpoons (H_7L^2)^{5-}$	51.40(6)
$(H_2L^1)^{6-} + 4H^+ \rightleftharpoons (H_6L^1)^{2-}$	47.71(5)	$(H_3L^2)^{9-} + 5H^+ \rightleftharpoons (H_8L^2)^{4-}$	62.42(6)
$(H_2L^1)^{6-} + 5H^+ \rightleftharpoons (H_7L^1)^{-}$	57.15(6)	$(H_3L^2)^{9-} + 6H^+ \rightleftharpoons (H_9L^2)^{3-}$	72.69(8)
$(H_2L^1)^{6-} + 6H^+ \rightleftharpoons (H_8L^1)$	65.92(7)	$(H_3L^2)^{9-} + 7H^+ \rightleftharpoons (H_{10}L^2)^{2-}$	82.25(8)
$(H_2L^1)^{6-} + 7H^+ \rightleftharpoons (H_9L^1)^{+}$	70.78(8)	$(H_3L^2)^{9-} + 8H^+ \rightleftharpoons (H_{11}L^2)^{-}$	90.8(1)
$(H_2L^1)^{6-} + 8H^+ \rightleftharpoons (H_{10}L^1)^{2+}$	75.37(9)	$(H_3L^2)^{9-} + 9H^+ \rightleftharpoons (H_{12}L^2)$	98.7(1)
$(H_4L^1)^{4-} + H^+ \rightleftharpoons (H_5L^1)^{3-}$	10.89(7)	$(H_6L^2)^{6-} + H^+ \rightleftharpoons H_7L^2)^{5-}$	11.62(7)
$(H_5L^1)^{3-} + H^+ \rightleftharpoons (H_6L^1)^{2-}$	10.47(7)	$(H_7L^2)^{5-} + H^+ \rightleftharpoons H_8L^2)^{4-}$	11.02(8)
$(H_6L^1)^{2-} + H^+ \rightleftharpoons (H_7L^1)^{-}$	9.44(7)	$(H_8L^2)^{4-} + H^+ \rightleftharpoons (H_9L^2)^{3-}$	10.27(9)
$(H_7L^1)^{-} + H^+ \rightleftharpoons (H_8L^1)$	8.77(8)	$(H_9L^2)^{3-} + H^+ \rightleftharpoons (H_{10}L^2)^{2-}$	9.56(9)
$(H_8L^1) + H^+ \rightleftharpoons (H_9L^1)^{+}$	4.86(9)	$(H_{10}L^2)^{2-} + H^+ \rightleftharpoons (H_{11}L^2)^{-}$	8.5(1)
$(H_9L^1)^{+} + H^+ \rightleftharpoons H_{10}L^1)^{2+}$	4.6(1)	$(H_{11}L^2)^{-} + H^+ \rightleftharpoons (H_{12}L^2)$	7.9(1)

* Values in parentheses are standard deviations on the last significant figure.

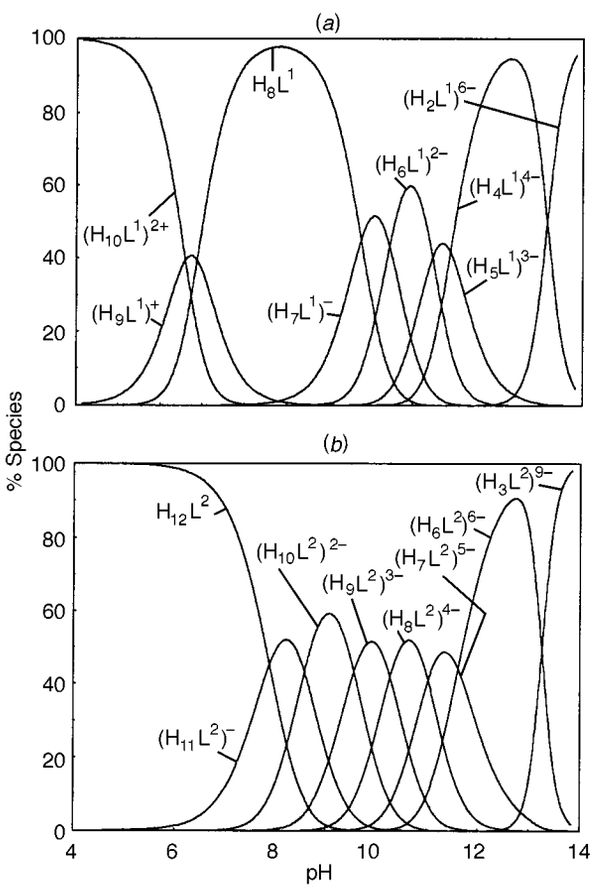

Fig. 3 Distribution diagrams of the protonated species formed by H_8L^1 (*a*) and $H_{12}L^2$ (*b*) as a function of pH. Macrocycle concentration 1×10^{-3} mol dm^{-3}, 0.1 mol dm^{-3} NMe_4Cl, 298.1 ± 0.1 K

catecholate anion determined under the present experimental conditions are log $K = 13.73(6)$, for $L^{2-} + H^+ \rightleftharpoons HL^-$ and 10.35(1) for $HL^- + H^+ \rightleftharpoons H_2L$. Accordingly, under the same conditions, the catechol derivatives $(L^1)^{8-}$ and $(L^2)^{12-}$ behave as very strong bases in the first protonation steps (Table 2). At pH 13.5, the upper limit of our pH-metric measurements, the two compounds are still present as diprotonated $(H_2L^1)^{6-}$ and triprotonated $(H_3L^2)^{9-}$ species, respectively, in which half of the catecholate groups are singly protonated. The successive addition of two protons to $(H_2L^1)^{6-}$ and three protons to $(H_3L^2)^{9-}$ cannot be resolved as separate single-proton transfers. The relevant equilibrium constants [log $K = 26.35(3)$ for $(H_2L^1)^{6-} + 2H^+ \rightleftharpoons (H_4L^1)^{4-}$ and 39.78(3) for $(H_3L^2)^{9-} + 3H^+ \rightleftharpoons (H_6L^2)^{6-}$] indicate that the very high basicity of the ligands persists until all catecholate groups are singly protonated (Table 2).

Also in the following protonation steps, leading to the formation of the H_8L^1 and $H_{12}L^2$, the anionic forms behave as considerably strong bases (Table 2). This is clearly evidenced by the distribution diagrams in Fig. 3 showing that the uncharged H_8L^1 and $H_{12}L^2$ start being formed in alkaline solutions and are almost the unique species at about pH 7. Compound H_8L^1, containing two tertiary amino groups, is able to bind two further protons giving rise to the cationic forms $(H_9L^1)^+$ and $(H_{10}L^1)^{2+}$.

Owing to the very high basicity of both compounds, the binding of protons is strongly competitive with the formation of metal complexes in solution. This made possible the determination of the iron(III) complex-formation constants by means of pH-metric titrations without competing ligands, in spite of the very high complex stabilities.

Complexation of Fe^{3+} by H_8L^1 and $H_{12}L^2$

The equilibrium constants for the iron(III) complexes are reported in Tables 3 and 4. Under the experimental conditions employed both ligands are capable of forming mono- and di-iron(III) complexes. As visualised by the concentration distribution curves of the complexes formed by H_8L^1 (Fig. 4) and $H_{12}L^2$ (Fig. 5), these molecules have a noticeable tendency to form dinuclear complexes, since even in a solution containing equimolar quantities of macrocycle and metal ion such species are formed in significant amounts over the whole pH range investigated, being the main complexes in very acidic solutions [Figs. 4(*a*), 5(*a*)]. Indeed, diiron(III) complexes are almost the unique species in solution at 2 : 1 metal to macrocycle molar ratios [Figs. 4(*b*), 5(*b*)].

In the limited pH ranges in which this complexation study was possible ($2.5 \leqslant pH \leqslant 5$ for H_8L^1 and $2.5 \leqslant pH \leqslant 9$ for $H_{12}L^2$, see Experimental section) no complexes containing the completely deprotonated ligands were observed, the mononuclear pentaprotonated $[Fe(H_5L^1)]$ and $[Fe(H_5L^2)]^{4-}$ and the dinuclear diprotonated species $[Fe_2(H_2L^1)]$ and $[Fe_2(H_2L^2)]^{4-}$ being the less protonated complexes formed around the upper limits of these pH ranges. On lowering the pH these complexes bind further protons in a stepwise mode till the species $[Fe(H_7L^1)]^{2+}$, $[Fe_2(H_6L^1)]^{4+}$, $[Fe(H_{10}L^2)]^+$ and $[Fe_2(H_2L^2)]^{4-}$ are formed. The protonation behaviour of such complexes, proceeding through sequential one-proton steps, can be attributed to the ability of the ligands to shift from catecholate to salicylate co-ordination modes. This behaviour is typical of enterobactin and tripodal analogues,[5b,6f,23,24] while the iron(III) complexes of ligands in which the carbonyl groups are not in the neighbourhood of the catechol rings, preventing salicylate-like chelation of the metal ion, double protonation and concomi-

Table 3 Logarithms of the equilibrium constants for the formation of mono- and di-nuclear complexes of Fe^{3+} with $(L^1)^{8-}$ determined in water–dmso (50 : 50 v/v), 0.1 mol dm^{-3} NMe_4Cl, at 298.1 ± 0.1 K

Reaction	log *K*
$Fe^{3+} + (H_2L^1)^{6-} + 3H^+ \rightleftharpoons [Fe(H_5L^1)]$	63.26(4) *
$Fe^{3+} + (H_2L^1)^{6-} + 4H^+ \rightleftharpoons [Fe(H_6L^1)]^+$	67.74(3)
$Fe^{3+} + (H_2L^1)^{6-} + 5H^+ \rightleftharpoons [Fe(H_7L^1)]^{2+}$	71.31(4)
$[Fe(H_5L)] + H^+ \rightleftharpoons [Fe(H_6L^1)]^+$	4.48(5)
$[Fe(H_6L)]^+ + H^+ \rightleftharpoons [Fe(H_7L^1)]^{2+}$	3.57(5)
$Fe^{3+} + (H_5L^1)^{3-} \rightleftharpoons [Fe(H_5L^1)]$	26.02(7)
$Fe^{3+} + (H_6L^1)^{2-} \rightleftharpoons [Fe(H_6L^1)]^+$	20.03(6)
$Fe^{3+} + (H_7L^1)^- \rightleftharpoons [Fe(H_7L^1)]^{2+}$	14.16(7)

Reaction	log *K*
$2Fe^{3+} + (H_2L^1)^{6-} \rightleftharpoons [Fe_2(H_2L^1)]$	58.08(6)
$2Fe^{3+} + (H_2L^1)^{6-} + H^+ \rightleftharpoons [Fe_2(H_3L^1)]^+$	62.0(1)
$2Fe^{3+} + (H_2L^1)^{6-} + 2H^+ \rightleftharpoons [Fe_2(H_4L^1)]^{2+}$	66.90(7)
$2Fe^{3+} + (H_2L^1)^{6-} + 3H^+ \rightleftharpoons [Fe_2(H_5L^1)]^{3+}$	69.52(7)
$2Fe^{3+} + (H_2L^1)^{6-} + 4H^+ \rightleftharpoons [Fe_2(H_6L^1)]^{4+}$	72.76(9)
$[Fe_2(H_2L^1)] + H^+ \rightleftharpoons [Fe_2(H_3L^1)]^+$	3.9(1)
$[Fe_2(H_3L^1)]^+ + H^+ \rightleftharpoons [Fe_2(H_4L^1)]^{2+}$	4.9(1)
$[Fe_2(H_4L^1)]^{2+} + H^+ \rightleftharpoons [Fe_2(H_5L^1)]^{3+}$	2.62(8)
$[Fe_2(H_5L^1)]^{3+} + H^+ \rightleftharpoons [Fe_2(H_6L^1)]^{4+}$	3.2(1)
$Fe^{3+} + [Fe(H_5L^1)] \rightleftharpoons [Fe_2(H_5L^1)]^{3+}$	6.26(8)
$Fe^{3+} + [Fe(H_6L^1)]^+ \rightleftharpoons [Fe_2(H_6L^1)]^{4+}$	5.0(1)

* Values in parentheses are standard deviations on the last significant figure.

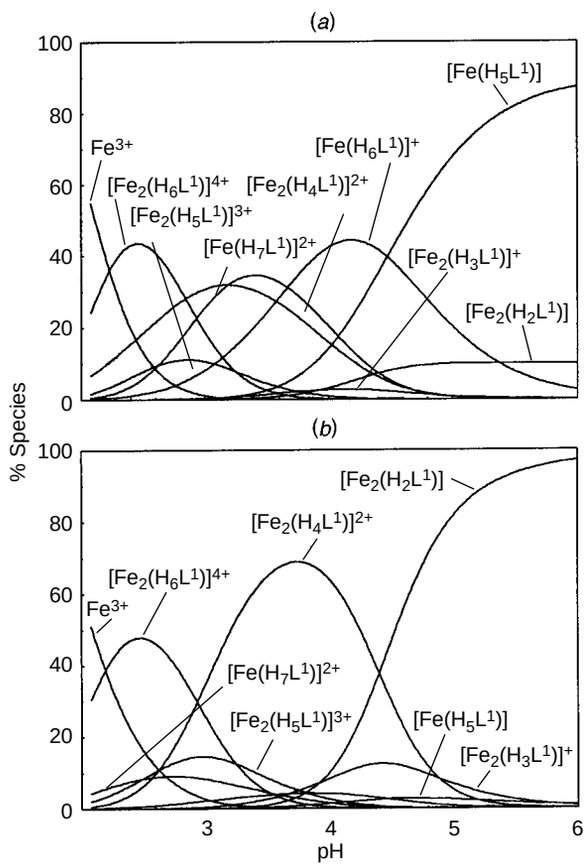

Fig. 4 Distribution diagrams of the protonated species formed in the system Fe^{3+}–H_8L^1. (*a*) $[H_8L^1] = [Fe^{3+}] = 1 \times 10^{-3}$ mol dm^{-3}, (*b*) $[H_8L^1] = 1 \times 10^{-3}$, $[Fe^{3+}] = 2 \times 10^{-3}$ mol dm^{-3}; 0.1 mol dm^{-3} NMe_4Cl, 298.1 ± 0.1 K

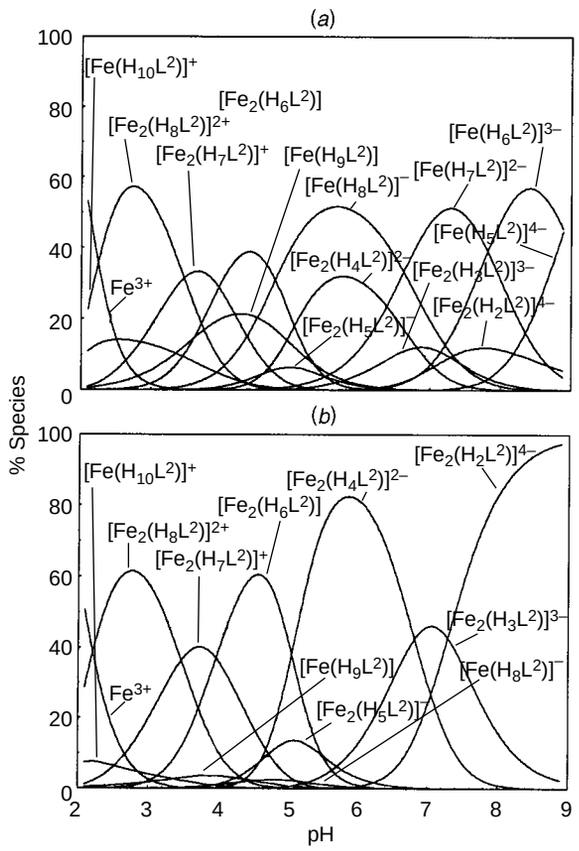

Fig. 5 Distribution diagrams of the protonated species formed in the system Fe^{3+}–$H_{12}L^2$. (*a*) $[H_{12}L^2] = [Fe^{3+}] = 1 \times 10^{-3}$ mol dm^{-3}, (*b*) $[H_{12}L^2] = 1 \times 10^{-3}$, $[Fe^{3+}] = 2 \times 10^{-3}$ mol dm^{-3}; 0.1 mol dm^{-3} NMe_4Cl, 298.1 ± 0.1 K

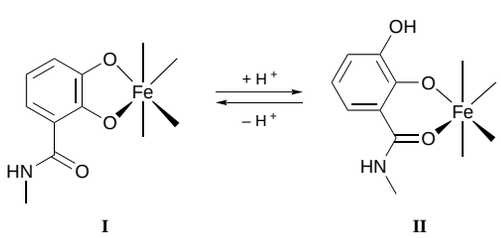

tant detachment of one catechol group from the metal centre occurs.[6f] Similar two-proton steps have been observed in the protonation reaction of iron(III) complexes of catechol-based cage-like ligands for which the change from catecholate to salicylate mode of bonding appears to be sterically inaccessible.[6i]

In the case of H_8L^1 also the possible protonation of the two methylated amino groups must be considered. For instance, since the equilibrium constant for the reaction of Fe^{3+} with $(H_7L^1)^-$ [log $K = 14.16(7)$] is almost equal to the equilibrium constant for $Fe^{3+} + (H_{10}L^2)^{2-}$ [log $K = 14.7(1)$] one should expect that both ligands involve the same number of donor atoms in these complexation reactions. Hence, considering that in $(H_{10}L^2)^{2-}$ there are only two unprotonated catechol oxygens available for complexation, at least one proton in $[Fe(H_7L^1)]^{2+}$ should be located on a ligand amino group. It seems reasonable that also in the dinuclear complexes formed by H_8L^1 in very acidic solutions one or two protons are bound to the methylated amino groups. For instance in $[Fe_2(H_6L^1)]^{4+}$ two protons should be on nitrogen atoms allowing four catecholate oxygens to be involved in the complexation of the two Fe^{3+} ions.

The equilibrium constants for the protonation of the dinuclear complexes (Tables 3 and 4) reveal a rather unusual

Table 4 Logarithms of the equilibrium constants for the formation of mono- and di-nuclear complexes of Fe^{3+} with $(L^2)^{12-}$ determined in water–dmso (50 : 50 v/v), 0.1 mol dm^{-3} NMe_4Cl, at 298.1 ± 0.1 K

Reaction	log *K*
$Fe^{3+} + (H_3L^2)^{9-} + 2H^+ \rightleftharpoons [Fe(H_5L^2)]^{4-}$	67.75(4) *
$Fe^{3+} + (H_3L^2)^{9-} + 3H^+ \rightleftharpoons [Fe(H_6L^2)]^{3-}$	74.65(4)
$Fe^{3+} + (H_3L^2)^{9-} + 4H^+ \rightleftharpoons [Fe(H_7L^2)]^{2-}$	82.46(4)
$Fe^{3+} + (H_3L^2)^{9-} + 5H^+ \rightleftharpoons [Fe(H_8L^2)]^{-}$	89.08(5)
$Fe^{3+} + (H_3L^2)^{9-} + 6H^+ \rightleftharpoons [Fe(H_9L^2)]$	93.60(5)
$Fe^{3+} + (H_3L^2)^{9-} + 7H^+ \rightleftharpoons [Fe(H_{10}L^2)]^{+}$	96.95(5)
$[Fe(H_5L^2)]^{4-} + H^+ \rightleftharpoons [Fe(H_6L^2)]^{3-}$	8.90(5)
$[Fe(H_6L^2)]^{3-} + H^+ \rightleftharpoons [Fe(H_7L^2)]^{2-}$	7.81(5)
$[Fe(H_7L^2)]^{2-} + H^+ \rightleftharpoons [Fe(H_8L^2)]^{-}$	6.62(6)
$[Fe(H_8L^2)]^{-} + H^+ \rightleftharpoons [Fe(H_9L^2)]$	4.52(6)
$[Fe(H_9L^2)] + H^+ \rightleftharpoons [Fe(H_{10}L^2)]^{+}$	3.35(6)
$Fe^{3+} + (H_6L^2)^{6-} \rightleftharpoons [Fe(H_6L^2)]^{3-}$	34.87(5)
$Fe^{3+} + (H_7L^2)^{5-} \rightleftharpoons [Fe(H_7L^2)]^{2-}$	31.06(6)
$Fe^{3+} + (H_8L^2)^{4-} \rightleftharpoons [Fe(H_8L^2)]^{-}$	26.66(7)
$Fe^{3+} + (H_9L^2)^{3-} \rightleftharpoons [Fe(H_9L^2)]$	20.91(9)
$Fe^{3+} + (H_{10}L^2)]^{-} \rightleftharpoons [Fe_2(H_{10}L^2)]^{+}$	14.7(1)
$2Fe^{3+} + (H_3L^2)^{9-} \rightleftharpoons [Fe_2(H_2L^2)]^{4-} + H^+$	64.41(4)
$2Fe^{3+} + (H_3L^2)^{9-} \rightleftharpoons [Fe_2(H_3L^2)]^{3-}$	71.70(5)
$2Fe^{3+} + (H_3L^2)^{9-} + H^+ \rightleftharpoons [Fe_2(H_4L^2)]^{2-}$	78.51(4)
$2Fe^{3+} + (H_3L^2)^{9-} + 2H^+ \rightleftharpoons [Fe_2(H_5L^2)]^{-}$	83.1(1)
$2Fe^{3+} + (H_3L^2)^{9-} + 3H^+ \rightleftharpoons [Fe_2(H_6L^2)]$	88.62(4)
$2Fe^{3+} + (H_3L^2)^{9-} + 4H^+ \rightleftharpoons [Fe_2(H_7L^2)]^{+}$	92.59(3)
$2Fe^{3+} + (H_3L^2)^{9-} + 5H^+ \rightleftharpoons [Fe_2(H_8L^2)]^{2+}$	96.06(4)
$[Fe_2(H_2L^2)]^{4-} + H^+ \rightleftharpoons [Fe_2(H_3L^2)]^{3-}$	7.29(6)
$[Fe_2(H_3L^2)]^{3-} + H^+ \rightleftharpoons [Fe_2(H_4L^2)]^{2-}$	6.81(6)
$[Fe_2(H_4L^2)]^{2-} + H^+ \rightleftharpoons [Fe_2(H_5L^2)]^{-}$	4.6(1)
$[Fe_2(H_5L^2)]^{-} + H^+ \rightleftharpoons [Fe_2(H_6L^2)]$	5.5(1)
$[Fe_2(H_6L^2)] + H^+ \rightleftharpoons [Fe_2(H_7L^2)]^{+}$	3.97(5)
$[Fe_2(H_7L^2)]^{+} + H^+ \rightleftharpoons [Fe_2(H_8L^2)]^{2+}$	3.47(5)
$Fe^{3+} + [Fe(H_5L^2)]^{4-} \rightleftharpoons [Fe_2(H_5L^2)]^{-}$	17.3(1)
$Fe^{3+} + [Fe(H_6L^2)]^{3-} \rightleftharpoons [Fe_2(H_6L^2)]$	13.97(5)
$Fe^{3+} + [Fe(H_7L^2)]^{2-} \rightleftharpoons [Fe_2(H_7L^2)]^{+}$	10.13(5)
$Fe^{3+} + [Fe(H_8L^2)]^{-} \rightleftharpoons [Fe_2(H_8L^2)]^{2+}$	6.98(5)

* Values in parentheses are standard deviations on the last significant figure.

behaviour, since they do not present a smooth decrease in the successive protonation steps. Nevertheless, this is not a very exotic feature and it is associated with complexes characterised by high intramolecular connectivity where each protonation step can produce important reorganisation of the complex structure, facilitating the binding of successive protons.

As evidenced by the species distribution curves in Figs. 4 and 5, H_8L^1 and $H_{12}L^2$ are efficient iron(III) ion sequestering agents, since even in solutions containing ligand and metal ion in 1 : 2 molar ratios all Fe^{3+} is complexed at about pH 3. Nevertheless, due to the concomitance of several complexation equilibria and to their pH dependence, these distribution diagrams, as well as the log *K* values of the complexes formed, are inadequate for a direct comparison of the iron-binding properties of similar ligands. In order to evaluate the potential ability of such ligands to scavenge iron(III) ion from the human iron stores it is preferable to consider the actual concentration of free Fe^{3+} in equilibrium with its complexed forms under given conditions. For this purpose the $[Fe(H_2O)_6]^{3+}$ concentration in aqueous solution containing 10^{-6} mol dm^{-3} total iron and 10^{-5} mol dm^{-3} total ligand at physiological pH, *i.e.* pH 7.4, is generally used. Table 5 lists several pM values {pM = −log $[Fe(H_2O)_6]^{3+}$} for natural and synthetic iron(III) ion binding agents.

On the base of the equilibrium constants reported in Table 4 it is possible to calculate a comparative pM value for $H_{12}L^2$ considering that pH 7.4 in pure water corresponds to pH 8.4 in water–dmso (50 : 50 v/v). The value obtained, pM 27.7, although presumably a few units greater than the values expected in pure water, seems to be large enough to ensure favourable competition (from a thermodynamic point of view) with transferrin (pM 23.6) in the binding of Fe^{3+}. In the case of H_8L^1 it is not possible to calculate a correct pM value, since the stability constants of the complexes formed at around pH 8.4 could not be determined (see Experimental section). Nevertheless, a very pessimistic estimation of pM (at pH 8.4) for this ligand can be made including in the calculation only the stability constants of the complexes formed in the pH range investigated (pH < 5), namely 23.4. In conclusion it seems reasonable that also H_8L^1 might be thermodynamically able to scavenge Fe^{3+} from iron(III) transferrin.

In order to verify the effectiveness of H_8L^1 and $H_{12}L^2$ as iron(III) ion sequestering agents in water, we followed by spectrophotometric measurements the transmetallation reactions occurring in the presence of these compounds and diiron(III) transferrin. The spectrophotometric study also furnished some information on the co-ordination environment

Table 5 pM Values for some natural and synthetic iron(III) ion binding agents

Ligand [a]	pM [b]
Enterobactin	35.5
HBED	31.0
Bicapped TRENCAM	30.7
MECAM	29.1
TRENCAM	27.8
$H_{12}L^2$	27.7 [c]
Desferrioxamine B	26.6
Ferrichrome A	25.2
H_5dtpa	24.7
Transferrin	23.6
H_8L^1	23.4 [c,d]
H_4edta	22.2

[a] H_4edta = Ethylenedinitrilotetraacetic acid, H_5dtpa = (carboxymethyl)-iminobis(ethylenedinitrilo)tetraacetic acid, HBED = *N*,*N*′-bis(2-hydroxybenzyl)-2,2′-(ethane-1,2-diyldiamino)diacetic acid, TRENCAM = tris[2-(2,3-dihydroxybenzamido)ethyl]amine, MECAM = tris(2,3-dihydroxybenzamidomethyl)benzene. [b] pM = −log $[Fe(H_2O)_6{}^{3+}]$ at pH 7.4 and 10^{-6} mol dm^{-3} total iron concentration, 10^{-5} mol dm^{-3} total ligand concentration, in water. [c] At pH 8.4 in water–dmso (50 : 50 v/v). [d] Extrapolated value (see text). Previous values taken from ref. 6(*f*,*h*,*i*).

of the metal ion. Spectra of solutions containing equimolar amounts of Fe^{3+} and $H_{12}L^2$ at pH > 10, exhibiting a maximum at 484 nm (ε 4175 dm^3 mol^{-1} cm^{-1}), are quite similar to those reported for the octahedral complex tris(catecholato)iron(III) (λ_{max} = 490, ε 4190 dm^3 mol^{-1} cm^{-1}),[25] in accordance with the involvement of three catecholate units of the ligand in iron(III) co-ordination at these pH values. Addition of a second equivalent of Fe^{3+} to 1 : 1 metal to macrocycle solutions at pH > 10 does not produce substantial changes of the spectral features with respect to the total concentration of the metal ion since 2 : 1 solutions show the same spectra as those of 1 : 1 solutions with double the iron(III) ion concentration (λ_{max} = 480 nm, ε 8300 dm^3 mol^{-1} cm^{-1} for 2 : 1 metal : macrocycle solutions). These observations indicate that $H_{12}L^2$ behaves as a ditopic ligand furnishing two tris(catecholato)-like lodgings for the formation of a diiron(III) complex.

A similar situation occurs for H_8L^1, as evidenced by the spectra of solutions containing Fe^{3+} and macrocycle in 1 : 1 (λ_{max} = 514, ε 3000) and 2 : 1 (λ_{max} = 510 nm, ε 5960 dm^3 mol^{-1} cm^{-1}) molar ratios at pH 10. The similarity of these spectra with that of bis(catecholato)iron(III) (λ_{max} = 570 nm, ε 3330 dm^3 mol^{-1} cm^{-1}),[25] and the structure of H_8L^1, accounts for

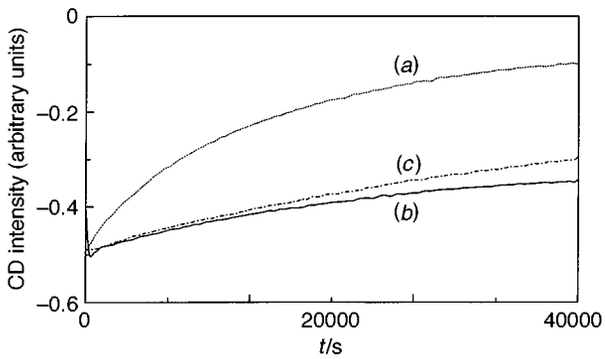

Fig. 6 Time dependence of the intensity of the negative dichroic band of iron transferrin (450 nm) following reactions with $H_{12}L^2$ (*a*), H_8L^1 (*b*) or desferrioxamine B (*c*). Diiron(III) transferrin concentration 5×10^{-5} mol dm^{-3}, phosphate buffer 0.1 mol dm^{-3}, pH 7.4, ligand concentration 2×10^{-4} mol dm^{-3}

the binding of each iron(III) ion to a couple of catecholate groups.

It is interesting that on addition of one catechol per iron(III) ion to the previous solutions containing H_8L^1 complexes, at pH 10, one obtains almost the same spectra as those observed for the octahedral complexes of $H_{12}L^2$ at the same pH.

Iron removal from diiron(III) transferrin by H_8L^1 and $H_{12}L^2$

Diiron(III) transferrin samples were treated with a two-fold excess of either macrocycle, and iron removal from the specific protein sites monitored through circular dichroism. In all cases the iron(III)-scavenging ability of the new compounds was compared to that of desferrioxamine B (Desferal), the only iron chelating agent presently used in clinical therapies.[26] It must be stressed that the use of CD is particularly appropriate in our case since it reveals only iron(III) bound to the protein, while the iron(III) ions bound to the ligand are CD silent.

Two individual sets of experiments were carried out to examine the iron-scavenging reaction. In the first one iron removal was monitored at pH 7.4 in the presence of 0.1 mol dm^{-3} Na_2SO_4, and 10 mmol dm^{-3} *N*′-(2-hydroxyethyl)piperazine-*N*-ethane-2-sulfonic acid (hepes); in the second the reaction was carried out in the presence of 0.1 mol dm^{-3} phosphate buffer, pH 7.4. Whereas in the former case the iron release was extremely slow with respect to all ligands (several days for each reaction), in the latter the reaction is significantly faster and reaches completion within 20–50 h. Time-dependence profiles for the reactions carried out in the presence of 0.1 mol dm^{-3} phosphate are shown in Fig. 6. It is apparent that the iron-removal reaction is much faster for $H_{12}L^2$ than for H_8L^1; under the same experimental conditions desferrioxamine B (DFB) is much less effective than $H_{12}L^2$ but slightly more effective than H_8L^1. The percentage of iron extraction after 10 h is 25% for H_8L^1, 30% for DFB and 80% for $H_{12}L^2$.

The fact that the iron extraction rates are very low in all cases, even in the presence of 0.1 mol dm^{-3} phosphate, implies that the various ligands (H_8L^1, $H_{12}L^2$ and DFB), unlike diphosphate and some phosphonate ligands, are not able to approach closely the protein-bound metal ion and remove it;[27,28] their inertness must probably be ascribed to their bulkiness and/or to their inability to induce local conformational changes of the iron binding site.[29] Thus, on the grounds of these results, it can be hypothesised that the mechanism of the iron-release reaction is predominantly dissociative even if not purely dissociative (indeed, the apparent extraction rates depend on the nature of the chelating agent). Conversely, the large increase in the iron-scavenging rates observed upon replacement of sodium sulfate with the phosphate buffer may be due either to modulation of the protein conformation by phosphate or to direct access of the phosphate group to protein-bound iron (according to a shuttle mechanism).

In any case, independently of the mechanism of iron release, it must be stressed here that both compounds are able to remove iron(III) from transferrin *in vitro* and that $H_{12}L^2$ is significantly more effective than DFB in doing so. A more extensive biological evaluation of these new compounds is now warranted for possible applications in iron-chelation strategies.

Acknowledgements

The authors are indebted to Mr. M. Fontanelli, Dr. P. Mariani, and Dr. S. Seniori Constantini for technical assistance. Financial support from the Italian Ministero dell'Università e della Ricerca Scientifica e Tecnologica (quota 60%), the Progetto Finalizzato di Chimica Fine e Secondaria of the Italian Research Council (CNR) is gratefully acknowledged.

References

1 *Iron Transport in Microbes, Plants and Animals*, eds. G. Winkelmann, D. Van der Helm and J. B. Neilands, VCH, Weinheim, 1987.
2 B. F. Matzanke, G. Müller-Matzanke and K. N. Raymond, in *Iron Carriers and Iron Proteins*, ed. T. M. Loehr, VCH, New York, 1989.
3 K. N. Raymond, *Coord. Chem. Rev.*, 1990, **105**, 135.
4 R. C. Hider, *Struct. Bonding* (*Berlin*), 1984, **58**, 25.
5 (*a*) W. R. Harris, C. J. Carrano and K. N. Raymond, *J. Am. Chem. Soc.*, 1979, **101**, 2213; (*b*) W. R. Harris, C. J. Carrano, S. R. Cooper, S. R. Sofen, A. E. Avdeef, J. V. McArdle and K. N. Raymond, *J. Am. Chem. Soc.*, 1979, **101**, 6097.
6 (*a*) F. L. Weitl and K. N. Raymond, *J. Am. Chem. Soc.*, 1979, **101**, 2728; (*b*) M. C. Venuti, W. H. Rastetter and J. B. Neilands, *J. Med. Chem.*, 1979, **22**, 123; (*c*) F. L. Weitl, K. N. Raymond and P. W. Durbin, *J. Med. Chem.*, 1981, **103**, 203; (*d*) W. R. Harris, F. L. Weitl and K. N. Raymond, *J. Chem. Soc.*, *Chem. Commun.*, 1979, 177; (*e*) F. L. Weitl, W. R. Harris and K. N. Raymond, *J. Med. Chem.*, 1979, **22**, 1281; (*f*) W. R. Harris, K. N. Raymond and F. L. Weitl, *J. Am. Chem. Soc.*, 1981, **103**, 2667; (*g*) T. J. McMurry, S. J. Rodger and K. N. Raymond, *J. Am. Chem. Soc.*, 1987, **109**, 3451; (*h*) V. L. Pecoraro, F. L. Weitl and K. N. Raymond, *J. Am. Chem. Soc.*, 1981, **103**, 5133; (*i*) T. M. Garrett, T. J. McMurry, M. W. Hosseini, Z. E. Reyes, F. E. Hahn and K. N. Raymond, *J. Am. Chem. Soc.*, 1991, **113**, 2965; (*k*) T. B. Karpishin, T. D. P. Stack and K. N. Raymond, *J. Am. Chem. Soc.*, 1993, **115**, 6115.
7 A. Shanzer, J. Libman, S. Lifson and C. E. Felder, *J. Am. Chem. Soc.*, 1986, **108**, 7609; Y. Tor, J. Libman, A. Shanzer and S. Lifson, *J. Am. Chem. Soc.*, 1987, **109**, 6517; Y. Tor, J. Libman and A. Shanzer, *J. Am. Chem. Soc.*, 1987, **109**, 6518; Y. Tor, J. Libman, A. Shanzer, C. E. Felder and S. Lifson, *J. Chem. Soc.*, *Chem. Commun.*, 1987, 749; Y. Tor, J. Libman, A. Shanzer, C. E. Felder and S. Lifson, *J. Am. Chem. Soc.*, 1992, **114**, 6661.
8 W. Kiggen and F. Vögtle, *Angew. Chem.*, *Int. Ed. Engl.*, 1984, **23**, 714; W. Kiggen, F. Vögtle, S. Franken and H. Puff, *Tetrahedron*, 1986, **42**, 1859; S. Stutte, W. Kiggen and F. Vögtle, *Tetrahedron*, 1987, **43**, 2065.
9 M. J. Kendrick, M. T. May, M. J. Plishka and K. D. Robinson, *Metals in Biological Systems*, Ellis Horwood, Chichester, 1992.
10 M. N. Hughes, *The Inorganic Chemistry of the Biological Processes*, Wiley, New York, 1981.
11 S. A. Kretchmar Nguyen, A. Craig and K. N. Raymond, *J. Am. Chem. Soc.*, 1993, **115**, 6758.
12 S. A. Chung and K. N. Raymond, *J. Am. Chem. Soc.*, 1993, **115**, 6758.
13 F. Lloret, J. Moratal and J. Faus, *An Quim. B*, 1981, **77**, 202; *J. Chem. Soc.*, *Dalton Trans.*, 1983, 1743, 1749; *An Quim.*, 1986, **82**, 34; F. Lloret, M. Mollar, J. Moratal and J. Faus, *Inorg. Chim. Acta*, 1986, **124**, 67; F. Lloret, M. Julve, M. Mollar, I. Castro, J. Latorre, J. Faus, X. Solans and I. Morgenstern-Badarau, *J. Chem. Soc.*, *Dalton Trans.*, 1989, 729; M. Mollar, I. Castro, F. Lloret, M. Julve, J. Faus and J. Latorre, *Transition Met. Chem.*, 1991, **16**, 31; F. Lloret, M. Mollar, J. Faus, M. Julve and I. Castro, *Inorg. Chim. Acta*, 1991, **189**, 195.
14 A. Andrés, C. Bazzicalupi, A. Bencini, A. Bianchi, V. Fusi, E. Garcia-España, C. Giorgi, N. Nardi, P. Paoletti, J. A. Ramirez and B. Valtancoli, *J. Chem. Soc.*, *Perkin Trans. 2*, 1994, 2367.
15 N. Walker and D. D. Stuart, *Acta Crystallogr.*, *Sect. A*, 1983, **39**, 158.
16 SIR 92, A. Altamore, G. Cascarano, C. Giacovazzo and A. Guagliardi, *J. Appl. Crystallogr.*, 1993, **26**, 343.
17 G. M. Sheldrick, SHELXL 93, University of Göttingen, 1993.

18 *International Tables for X-Ray Crystallography*, Kynoch Press, Birmingham, 1974, vol. 4.
19 (*a*) A. Bianchi, L. Bologni, P. Dapporto, M. Micheloni and P. Paoletti, *Inorg. Chem.*, 1984, **23**, 1201; (*b*) A. Bencini, A. Bianchi, E. Garcia-España, M. Micheloni and P. Paoletti, *Inorg. Chem.*, 1988, **27**, 176.
20 G. Gran, *Analyst* (*London*), 1952, **77**, 661; F. J. Rossotti and H. Rossotti, *J. Chem. Educ.*, 1965, **42**, 375.
21 P. Gans, A. Sabatini and A. Vacca, *Talanta*, 1996, **43**, 1739.
22 C. K. Johnson, ORTEP, Report ORNL-3794, Oak Ridge National Laboratory, Oak Ridge, TN, 1971.
23 M. E. Cass, T. M. Garrett and K. N. Raymond, *J. Am. Chem. Soc.*, 1989, **111**, 1677.
24 W. R. Harris and K. N. Raymond, *J. Am. Chem. Soc.*, 1979, **101**, 6534.
25 A. Avdeef, S. R. Sofen, T. L. Bregante and K. N, Raymond, *J. Am. Chem. Soc.*, 1978, **100**, 5362.
26 S. Pollack, P. Aisen, F. D. Lasky and G. Vanderhoff, *Br. J. Haematol.*, 1976, **34**, 231.
27 W. R. Harris, *J. Inorg. Biochem.*, 1984, **21**, 263.
28 A. Egyed, *Biochim. Biophys. Acta*, 1975, **411**, 349; I. Bertini, J. Hirose, C. Luchinat, L. Messori, M. Piccioli and A. Scozzafava, *Inorg. Chem.*, 1988, **27**, 2405.
29 Z. Hou, D. W. Whisenhunt, J. Xu and K. N. Raymond, *J. Am. Chem. Soc.*, 1994, **116**, 840.

Received 23*rd September* 1997; *Paper* 7/06883B